Tunable fluid-solid metamaterials for manipulation of elastic wave propagation in broad frequency range

Quan Zhang, Kai Zhang, and Gengkai Hu

Citation: Appl. Phys. Lett. **112**, 221906 (2018); doi: 10.1063/1.5023307
View online: https://doi.org/10.1063/1.5023307
View Table of Contents: http://aip.scitation.org/toc/apl/112/22
Published by the American Institute of Physics

Tunable fluid-solid metamaterials for manipulation of elastic wave propagation in broad frequency range

Quan Zhang, Kai Zhang,[a] and Gengkai Hu
School of Aerospace Engineering, Beijing Institute of Technology, Beijing 100081, China

(Received 23 January 2018; accepted 21 May 2018; published online 1 June 2018)

Most current strategies for designing tunable locally resonant metamaterials are based on tuning the stiffness of the resonator; however, this approach presents a major shortcoming as the effective mass density is constant at a high frequency. Here, this paper reports a type of tunable locally elastic metamaterial—called "tunable fluid-solid composite." The proposed metamaterial consists of several liquid or gas inclusions in a solid matrix, controlled through a pair of embedded pumps. Both the band gap and effective mass density at the high frequency can be tuned by controlling the liquid distribution in the unit cell, as demonstrated through a combination of theoretical analysis, numerical simulation, and experimental testing. Finally, we show that the tunable fluid-solid metamaterial can be utilized to manipulate wave propagation over a broad frequency range, providing avenues for vibration isolation and wave guiding. *Published by AIP Publishing.*
https://doi.org/10.1063/1.5023307

Elastic metamaterials have attracted significant interest in recent years because of their broad range of applications, including vibration isolation,[1,2] wave guiding,[3–6] cloaking,[7–11] and focusing.[12–14] Practically, owing to their fixed microstructure, traditional elastic metamaterials only operate over fixed frequency ranges, which limit additional potential applications. To address this issue, electromagnets,[4,15] shape memory effect,[16] structural deformation,[17,18] fluid-structure interaction,[19] and piezo-shunting[20,21] have been employed to achieve elastic metamaterials with tunable band gaps. Essentially, tunable locally resonant metamaterials can be divided into two types: those obtained by tuning the stiffness and those realized by tuning the resonator mass. Currently, most strategies for designing tunable locally resonant metamaterials are based on the former approach. However, challenge still remains, that is, the effective mass density of locally resonant metamaterials tuned by changing resonator stiffness is constant at a high frequency,[22] contrary to the requirements of the transformation method based on density regulation.

Theoretically, the effective mass density of locally resonant metamaterials at a high frequency is simply determined by the substrate mass and can be easily tuned if the mass distribution between the resonator and substrate can be modified. However, until now, no studies have investigated the control of mass distribution in the unit cell of elastic metamaterials. The main difficulty is that most elastic metamaterials are solid, resulting in a fixed constant mass distribution upon fabrication. Recently, Wang *et al.* indicated that the band gaps and transmission properties can be tuned by the selectively fluid filling of holes or hollow pillars in a solid phononic crystal.[23,24] In these works, the mass of the resonator can be tuned. Here, a type of tunable elastic metamaterial, called "tunable fluid-solid composite (tunable multiphase composite)," is developed. The proposed tunable fluid-solid composite (tunable multiphase composite) is based on a solid matrix containing several liquid or gas inclusions whose distributions can be easily tuned by controlling a central pump. Thus, the composite can be concretely applied to design tunable band gaps and effective mass density by controlling the liquid distribution in the unit cell. This study provides a perspective for the design of tunable metamaterials based on the concept of tunable fluid-solid composite, which can be applied to vibration isolation, wave guiding, and cloaking.

Effective mass density can be used to describe and predict wave propagation in elastic metamaterials.[25] Combined with the transformation method,[22] the propagation of an elastic wave along a designed path can be realized by tailoring the effective mass density, as shown in Fig. 1(a). Considering a typical locally resonant metamaterial [Fig. 1(a)], the effective mass density can be estimated through Lorentz model[25]

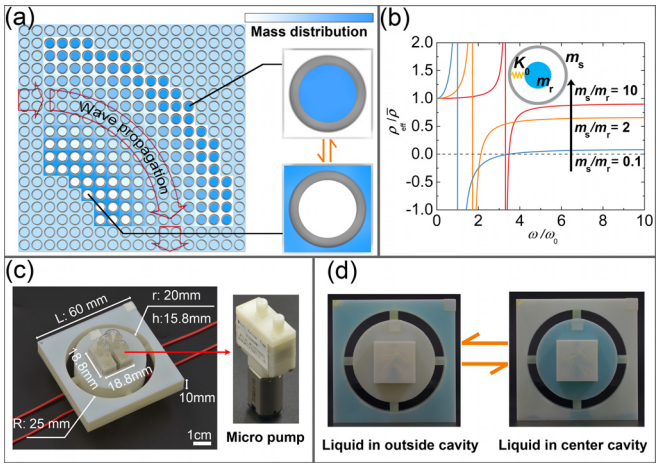

FIG. 1. Designed tunable locally resonant metamaterials. (a) Manipulation of wave propagation along a designed path by controlling mass distribution in different unit cells. (b) Effective mass density at different mass ratios between the substrate and resonator. (c) Dimensions of the designed unit cell, scale bar is 1 cm. The inset shows the micropump. (d) The liquid is transferred between central and external cavities by the pumps.

[a]zhangkai@bit.edu.cn

$$\rho_{\text{eff}} = \left[\frac{(\omega/\omega_0)^2}{1+r-(\omega/\omega_0)^2} \times \frac{1}{1+r} + 1\right]\bar{\rho}, \tag{1}$$

where $r = m_s/m_r$ (m_s and m_r are the masses of substrate and resonator, respectively), $\omega_0 = \sqrt{K_0/M_0}$ ($M_0 = m_s + m_r$ is a constant; K_0 is the stiffness of the resonator), and $\bar{\rho} = M_0/V$ (V is the effective volume of the unit cell). Figure 1(b) shows the relationships between $\rho_{\text{eff}}/\bar{\rho}$ and ω/ω_0 for different values of r. Notably, by controlling the mass distribution between m_s and m_r, the band gap of the lattice structure, which corresponds to the frequency range in which the effective mass density is negative, can be significantly altered. Furthermore, the effective mass density at a high frequency varies with r. Therefore, controlling the mass distribution between the resonator and substrate not only changes the locally resonant band gap but also allows altering the effective mass density at the high frequency, providing a promising approach to design tunable locally resonant metamaterials.

To realize this theoretical design, a pair of cavities are initially built by using a three-dimensional (3D) printer (Object 350, Stratasys, USA) with a photosensitive resin [RGD835, VeroWhitePlus, Stratasys, USA; Young's modulus $E = 2$ GPa, which varies little with the increase in frequency at room temperature;[26] density $\rho = 1200\ \text{kg m}^{-3}$; and Poisson's ratio is assumed to be 0.33; Figs. 1(c) and 1(d)]. The wall thickness t of the pair of cavities is equal to 0.7 mm, while the other geometrical dimensions are shown in Fig. 1(c). To build the unit cell, the cavities are connected through four tubes (outer diameter: 4.0 mm; inner diameter: 2.0 mm) made of silicon elastomer with Young's modulus $E_r = 20$ MPa and density $\rho_r = 500\ \text{kg m}^{-3}$. We prove that the variation of Poisson's ratio of the tube between 0.33 and 0.49 has little effect on the dispersion curves, as shown in the supplementary material. Finally, two micro pumps, used to transfer the liquid between the two cavities, are glued and embedded into the central cavity. Two tubules connect each pump with the central and external cavities. The total mass of the pumps, attached tubules, and thin lids is 15.72 g. To ensure that the liquid can be completely transferred from one cavity to the other, the volumes of the central and external cavities are designed to be equal. The central cavity, together with the pumps and tubes, acts as a local resonator, while the outside cavity behaves as a substrate. When the mass distribution of liquid in the central and external cavities is tuned, the mass of the local resonator changes. As a consequence, the natural frequency of the resonator will vary, determining the frequency range of the local resonance band gap.

In this work, a numerically based effective medium method[22] is also used to determine the out-of-plane effective mass density of the designed elastic metamaterial. In the numerical simulation, by applying the time-harmonic displacement constraints with $u = 0$, $v = 0$, and $w = Ae^{i\omega t}$ on the external surrounding boundaries of the unit cell, the effective mass density can be expressed as

$$\rho_{\text{eff}} = -\frac{F_z}{\omega^2 A V_{\text{eff}}}, \tag{2}$$

where F_z is the amplitude of the effective resultant force, V_{eff} is the effective volume of the unit cell, and A and ω are the amplitude and angular frequency of the applied displacement, respectively.

Figure 2(a) shows that the out-of-plane effective mass density of the proposed tunable elastic metamaterial can be affected by the liquid distribution in the unit cell. Numerical calculations on the effective mass density of the metamaterial shows very good agreement with the results estimated through Eq. (1). For a given time-harmonic displacement, the interaction force between the resonator and substrate, which contributes to the total effective resultant force (F_z), varies with the mass of the resonator. Therefore, controlling the liquid distribution between the resonator and substrate through embedded pumps results in different amplitudes of effective resultant force of the unit cell [Eq. (2)], further tailoring the effective mass density of the proposed metamaterial.

To validate the theoretical and numerical predictions, a sample consisting of 10×1 unit cells is fabricated. In the experimental setup shown in Fig. 2(c), the plane wave vibrating in the out-of-plane direction is excited by an electrodynamic shaker (HEV-50, Nanjing Foneng, China), which is directly connected to one end of the sample to provide harmonic signal over a broadband frequency range. The dynamic responses at different frequencies are recorded by using two displacement sensors (IL-30, KEYENCE, Japan) attached at both ends of the sample. The transmittance is computed as the ratio between output and input displacement signals, written as $20\log_{10}\|A_{\text{out}}(\omega)/A_{\text{in}}(\omega)\|$.

Figure 2(b) shows the experimentally measured transmittance curves for three cases, i.e., liquid distributed in center cavity, liquid distributed in outside cavity, liquid

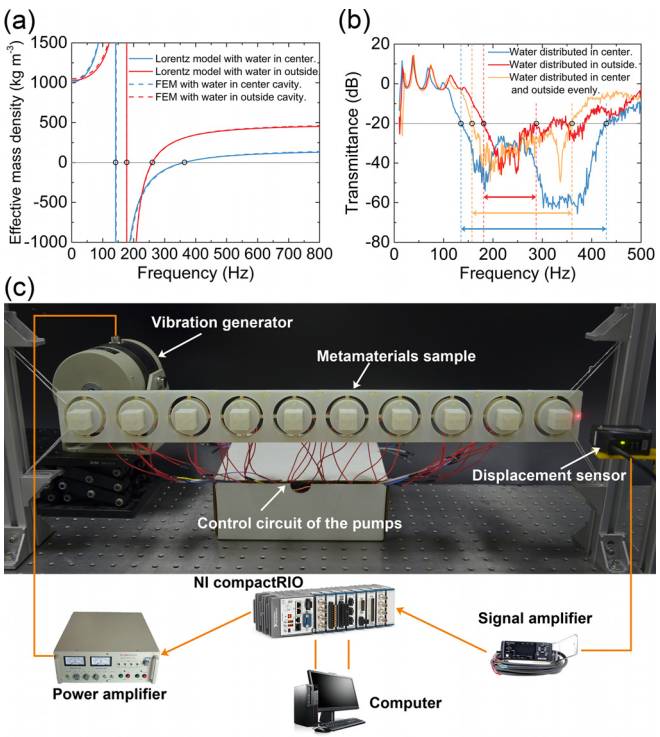

FIG. 2. (a) Calculated out-of-plane effective mass density of the proposed tunable fluid-solid metamaterial. (b) Experimental transmittance curves of the sample comprising 10×1 unit cells for different liquid distributions. (c) Experimental setup for the measurement of transmittance curves.

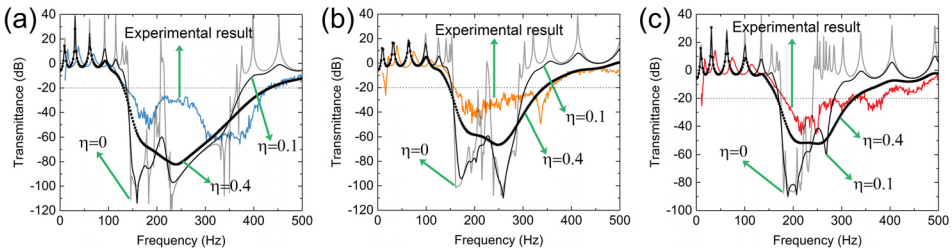

FIG. 3. The calculated transmittance curves for (a) liquid distributed in the center cavity, (b) liquid distributed evenly in the center and outside cavities, and (c) liquid distributed in the outside cavity. $\eta = 0$ corresponds to the numerical result without the effect of material damping.

distributed evenly in center and external cavities, respectively. In order to quantitatively compare the stopbands on the measured transmittance curves with the predicted band gaps in Fig. 2(a), according to the previous references,[17,19,27–29] the measured bandwidth is defined by selecting a specific attenuation value as a sufficient vibration attenuation threshold. Here, the attenuation value is chosen to be 20 dB, which is also used in relevant literatures.[17,27] The defined stop bands are marked by the two-headed arrows in Fig. 2(b). It should be noted that for the case water is distributed in the outside cavity (red curve), the transmittance fluctuates slightly around −20 dB over the frequency range from 287 Hz to 385 Hz, we select the first point (287 Hz) reaches −20 dB as the upper boundary of the stop band.

As shown in Fig. 2(b), the lower boundary of the stop band for liquid distributed in the outside cavity is 181 Hz, which matches well with the resonant frequency of 177 Hz, as predicted in Fig. 2(a) (the singular point of the red curve). When liquid is transferred into the center cavity, the lower boundary of the stop band defined from the measured transmittance curve changes to be 135 Hz, which also matches well with the predicted resonant frequency of 143 Hz, as shown in Fig. 2(a). On the other hand, the gap width on the measured transmittance curve for liquid distributed in the outside cavity is 106 Hz, wider than the predicted gap width of 84 Hz [the frequency range with the negative mass density as shown in Fig. 2(a)]. Similarly, the gap width on the measured transmittance curve for liquid distributed in the center cavity (294 Hz) is also wider than the predicted gap width (222 Hz). According to Ref. 30, the difference is mainly caused by the damping of the elastomer tubes which are used to connect the cavities. The damping of the resonator decreases the attenuation over the band gap and increases the attenuation over the frequency range beyond the band gap. To verify it, we also calculate the numerical transmittance curves with the effect of the structural damping coefficient of the elastomer tubes, as shown in Fig. 3. The acoustic-solid interaction module of COMSOL Multiphysics is adopted in the simulations. When the structural damping coefficient η is 0.4,[27,31,32] the overall trend of the measured transmittance curve coincides with that of the calculated one. However, the measured attenuation degree is much smaller than that of the calculated one for the frequency range from 175 to 290 Hz [see Fig. 3(a)]. In contrast, the measured attenuation degree significantly increases from 290 to 380 Hz on the blue curve. In the experiment, the electrodynamic shaker will cause vibration in the in-plane direction since it is not ideally perpendicular to the surface of the structure. For the frequency range located in stopband that is only related to the out-of-plane polarized modes (see the dispersion analysis below), the generated vibration in the in-plane direction will cause the variation of sensor reading, further reducing the measured attenuation degree. However, the effect of the in-plane vibration on the measured attenuation degree at the frequency located in the complete stopband (see the dispersion analysis below) vanishes.

In the proposed tunable locally resonant metamaterials, liquid distribution not only affects the elastic wave vibrating along the out-of-plane direction but it also perturbs the elastic wave vibrating along the in-plane direction. To further demonstrate this assertion, we conduct the dispersion analysis[33] through Finite Element Method (the acoustic-solid interaction module of COMSOL Multiphysics). Figures 4(a) and 4(b) show the band structure diagrams that correspond to the out-of-plane polarized modes and in-plane polarized modes for the case in which the liquid is completely distributed in the outside cavity, respectively. In contrast, at the right of each band structure diagram, the transmission spectrum of a finite sample consisting of 10×1 unit cells is presented. The frequency range with strong attenuation is consistent with the predicted band gap. On the other hand, when the liquid is transferred from the external to the central cavity, the effect of the mass distribution on the propagation of elastic waves is shown in Figs. 4(c) and 4(d). For each translational vibration mode of the resonator [shown in Figs. 4(c) and 4(d)], the corresponding natural frequency reduces, as the mass of the resonator increases while the stiffness

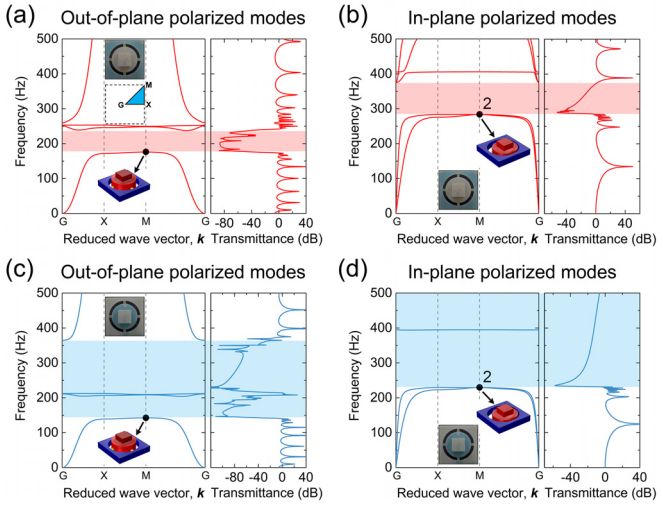

FIG. 4. Dispersion curves and numerical transmittance curves that correspond to (a) out-of-plane polarized modes and (b) in-plane polarized modes, respectively, for liquid distribution in the outside cavity. Dispersion curves and numerical transmittance curves that correspond to (c) out-of-plane polarized modes and (d) in-plane polarized modes, respectively, for liquid distribution in the center cavity.

remains unchanged. Moreover, the frequency ranges of the band gaps become wider as a result of the increase in mass ratio between the resonator and substrate. For each polarized modes, the stop bands on the band structure and transmission spectrum are also identical. In addition, for liquid distributed in the center cavity, there is a complete bandgap from 230 to 365 Hz [the overlap frequency range between Figs. 4(c) and 4(d)]. Meanwhile, the frequency range from 143 to 230 Hz is the band gap only related to the out-of-plane polarized modes. This confirms the previous explanation about the disagreement between the experimental and calculated transmittance curves. Notably, the unit cell dispersion analysis is scale invariant;[34] therefore, the findings of this work can be applied at different length scales.

The main function of liquid in our design is being controlled to change the mass distribution between the resonator and substrate. Here, the nonlinear dynamic behaviors play a weak role in our experiments. In our experiments, for the cases that liquid is distributed in only one cavity, there is no nonlinear dynamic behavior induced by the slosh of liquid since the liquid fully fills the cavity. For the case that liquid is distributed evenly in the center and external cavities, the vibration amplitude is kept to be very small in our experiment. Furthermore, the measured transmittance curve for this case is consistent with the simulated one (where the nonlinear dynamic effect is neglected). For an arbitrary liquid distribution state which is not involved in our experiments, the slosh of liquid can be avoided to a great extend through partitioning the cavity, as illustrated in the supplementary material.

In tuning methods based on tuning the stiffness of the resonator such as piezo-shunting, the frequency range over which the effective mass density meets the requirement of the transformation method is limited, as the effective mass density is constant at a high frequency.[22] Conversely, in our proposed tunable fluid-solid composite, the effective mass density at the high frequency can be tuned by controlling the mass distribution in the unit cell; this can be utilized to manipulate the wave propagation through a transformation method based on density regulation, as demonstrated in the supplementary material. Besides, the band gap can be conveniently broadened by choosing different liquid materials, for example, when water is replaced with other liquids (for example, liquid metal), the tuning ranges of the band gap can be significantly broadened, the relevant numerical results are also shown in the supplementary material.

In summary, we proposed a type of tunable elastic metamaterial—called "tunable fluid-solid composite." Both numerical and experimental results indicate that the band gaps of the proposed metamaterials can be tuned by controlling the liquid distribution in the unit cells. Compared with the current strategies based on tuning the stiffness of the resonator, our method provides remarkable advantages as the effective mass density at the high frequency can be tuned by controlling the mass distribution. This fluid-solid metamaterial can be applied to flexible structures, providing a better perspective for the design of intelligent systems for vibration isolation and waveguide.

See supplementary material for details on numerical transmittance curves, calculation of dispersion curves, waveguide design, and simulations.

This work has been supported by the National Natural Science Foundation of China (Grants Nos. 11672037, 11290153, and 11632003).

[1]J. Mei, G. Ma, M. Yang, Z. Yang, W. Wen, and P. Sheng, Nat. Commun. **3**, 756 (2012).
[2]D. Elser, U. L. Andersen, A. Korn, O. Glockl, S. Lorenz, C. Marquardt, and G. Leuchs, Phys. Rev. Lett. **97**, 133901 (2006).
[3]O. R. Bilal, A. Foehr, and C. Daraio, Adv. Mater. **29**, 1700628 (2017).
[4]Z. Wang, Q. Zhang, K. Zhang, and G. Hu, Adv. Mater. **28**, 9857 (2016).
[5]F. Casadei, T. Delpero, A. Bergamini, P. Ermanni, and M. Ruzzene, J. Appl. Phys. **112**, 064902 (2012).
[6]M. Kafesaki, M. M. Sigalas, and N. Garcia, Phys. Rev. Lett. **85**, 4044 (2000).
[7]L. Zigoneanu, B.-I. Popa, and S. A. Cummer, Nat. Mater. **13**, 352 (2014).
[8]S. A. Cummer and D. Schurig, New J. Phys. **9**, 45 (2007).
[9]M. Farhat, S. Guenneau, and S. Enoch, Phys. Rev. Lett. **103**, 024301 (2009).
[10]B.-I. Popa, L. Zigoneanu, and S. A. Cummer, Phys. Rev. Lett. **106**, 253901 (2011).
[11]M. K. Lee and Y. Y. Kim, Sci. Rep. **6**, 20731 (2016).
[12]R. Zhu, C. Ma, B. Zheng, M. Y. Musa, L. Jing, Y. Yang, H. Wang, S. Dehdashti, N. X. Fang, and H. Chen, Appl. Phys. Lett. **110**, 113503 (2017).
[13]G. Memoli, M. Caleap, M. Asakawa, D. R. Sahoo, B. W. Drinkwater, and S. Subramanian, Nat. Commun. **8**, 14608 (2017).
[14]M. Ambati, N. Fang, C. Sun, and X. Zhang, Phys. Rev. B **75**, 195447 (2007).
[15]O. R. Bilal, A. Foehr, and C. Daraio, Proc. Natl. Acad. Sci. U. S. A. **114**, 4603 (2017).
[16]Q. Zhang, D. Yan, K. Zhang, and G. Hu, Sci. Rep. **5**, 8936 (2015).
[17]S. Babaee, N. Viard, P. Wang, N. X. Fang, and K. Bertoldi, Adv. Mater. **28**, 1631 (2016).
[18]P. Wang, F. Casadei, S. Shan, J. C. Weaver, and K. Bertoldi, Phys. Rev. Lett. **113**, 014301 (2014).
[19]F. Casadei and K. Bertoldi, J. Appl. Phys. **115**, 034907 (2014).
[20]A. Bergamini, T. Delpero, L. D. Simoni, L. D. Lillo, M. Ruzzene, and P. Ermanni, Adv. Mater. **26**, 1343 (2014).
[21]Y. Chen, G. Hu, and G. Huang, J. Mech. Phys. Solids **105**, 179 (2017).
[22]Y. Chen, J. Hu, and G. Huang, J. Intell. Mater. Syst. Struct. **27**, 1337 (2016).
[23]Y.-F. Wang, T.-T. Wang, Y.-S. Wang, and V. Laude, Phys. Rev. Appl. **8**, 014006 (2017).
[24]T.-T. Wang, Y.-F. Wang, Y.-S. Wang, and V. Laude, Appl. Phys. Lett. **111**, 041906 (2017).
[25]X. N. Liu, G. K. Hu, C. T. Sun, and G. L. Huang, J. Sound Vib. **330**, 2536 (2011).
[26]M. Wagner, T. Chen, and K. Shea, 3D Print. Addit. Manuf. **4**(3), 133 (2017).
[27]D. Yu, Y. Liu, H. Zhao, G. Wang, and J. Qiu, Phys. Rev. B **73**, 064301 (2006).
[28]R. Zhu, X. N. Liu, G. K. Hu, C. T. Sun, and G. L. Huang, J. Sound Vib. **333**, 2759 (2014).
[29]P. Wang, Y. Zheng, M. C. Fernandes, Y. Sun, K. Xu, S. Sun, S. H. Kang, V. Tournat, and K. Bertoldi, Phys. Rev. Lett. **118**, 084302 (2017).
[30]Y. Y. Chen, M. V. Barnhart, J. K. Chen, G. K. Hu, C. T. Sun, and G. L. Huang, Compos. Struct. **136**, 358 (2016).
[31]R. S. Lakes, *Viscoelastic Materials* (Cambridge University Press, New York, USA, 2009), p. 208.
[32]R. S. Lakes, Phys. Rev. Lett. **86**, 2897 (2001).
[33]A. S. Phani, J. Woodhouse, and N. A. Fleck, J. Acoust. Soc. Am. **119**, 1995 (2006).
[34]O. R. Bilal, A. Foehr, and C. Daraio, Extreme Mech. Lett. **15**, 103 (2017).